//FS2/CUP/3-PAGINATION/DEX/2-PROOFS/3B2/9780521870283C05.3D 74 [74–98] 19.11.2007 9:27AM

5

Extensive summer hot and cold extremes under current and possible future climatic conditions: Europe and North America

ALEXANDER GERSHUNOV AND HERVÉ DOUVILLE

Condensed summary

The spatial scale of a heat wave is an important determinant of its impacts. Extensive summer hot and cold spells in Europe and North America are studied through observations and coupled model projections. Recent trends towards more frequent and extensive hot spells as well as rarer and less extensive cold outbreaks follow global warming trends, but they are regionally modulated on decadal timescales. Coupled model projections reflect these natural and anthropogenic influences, with their relative contributions depending on the particular scenarios assumed for global socioeconomic development. Europe appears to have had an early warning in 2003 of conditions that are projected for the second half of the twenty-first century, assuming a "business as usual" emissions scenario. North America, on the other hand, in spite of a general summer warming, has not seen the extent of summer heat that it can potentially experience even if global emissions of carbon dioxide and sulfate aerosols remain fixed at their current levels. Extensive and persistent heat waves naturally occur in association with widespread drought. The recent warming over North America is unusual in that it has occurred without the large-scale encouragement of a dry soil associated with precipitation deficit. Regional precipitation anomalies, together with global anthropogenic influences, can explain the atypical spatial pattern of recent North American summer warming. A decrease of precipitation to more normal amounts over the central and eastern United States is expected to result in a substantial summer warming over that region. Drought has the potential to seriously exacerbate the recent warming over North America to levels more in line with the warmest current model projections. Assuming realistic warming scenarios, a long-term anthropogenic increase (decrease) in the frequency and spatial extent of regional hot (cold) spells is projected to be strong and strongly modulated by decadal-scale variability throughout the twenty-first century.

Climate Extremes and Society, ed. H. F. Diaz and R. J. Murnane. Published by Cambridge University Press. © Cambridge University Press 2008.

//FS2/CUP/3-PAGINATION/DEX/2-PROOFS/3B2/9780521870283C05.3D 75 [74–98] 19.11.2007 9:27AM

5.1 Introduction

Outbreaks of anomalous summer heat occur each year somewhere on Earth. Typically associated with persistent blocking anticyclones, summertime heat waves in the mid-latitudes have a coherent spatial structure that is characterized by lack of rainfall, dry air and soil, and increased fire risk. Disastrous consequences (Macfarlane and Waller, 1976; Sheridan and Kalkstein, 2004) can result from hot spells that are extreme in their duration and spatial extent. The summer of 2003, very likely the hottest in at least 500 years (Luterbacher *et al.*, 2005), brought periods of sustained temperatures exceeding 35 °C over much of western and central Europe. The heat wave was accompanied by an almost complete lack of rainfall (Levinson and Waple, 2004), which resulted in wide-ranging environmental degradation, including severe impacts on agriculture, river flow, mountain glaciers, energy production, and toxicity (e.g., Beniston and Diaz, 2004), as well as wildfires in southwestern Europe, and over 10,000 heat-stress-related deaths in France alone (Levinson and Waple, 2004; Dhainaut *et al.*, 2004).

The Dust Bowl of the 1930s (Schubert *et al.*, 2004), a period of summertime heat and drought affecting large parts of North America – sustained over a decade and punctuated by exceptionally intense and extensive heat outbreaks in 1934, 1936, and 1937 – saw widespread hardship, farmland abandonment, and migration. Even mild hot spells of large spatial extent can cause havoc in the energy sector as demand for air conditioning rises beyond the capacity of power utilities to provide the needed electricity. Power outages during heat waves can lead to still higher human mortality through exposure. However, with adequate infrastructure in place, the health effects of heat waves can be effectively mitigated if the heat wave is anticipated even in the short term (Palecki *et al.*, 2001; Sheridan and Kalkstein, 2004).

Economic hardships (Subak *et al.*, 2000) due to unanticipated and unmitigated heat waves can result from rising power costs, as well as from decreased crop yields and increased livestock mortality. Environmental consequences of hot spells can range from loss of flora and fauna due directly to heat stress and indirectly by fire to depletion of natural water reservoirs and streamflow through related precipitation deficit and increased evaporation. Sustained hot spells can increase the risk of vector-borne and other infectious diseases (Ballester *et al.*, 2003; Zell, 2004). The larger the spatial extent of a heat wave, the more the related hydrologic deficit should be able to exert a positive feedback prolonging the condition.

The spatial scale of a heat wave is an important determinant of its environmental, economic, and health impacts. The scale of effort required to mitigate

//FS2/CUP/3-PAGINATION/DEX/2-PROOFS/3B2/9780521870283C05.3D 76 [74–98] 19.11.2007 9:27AM

these impacts also depends in large part on the event's spatial extent. Yet the scale parameter has been largely overlooked in climatological studies of heat waves. Extensive summer cold spells, although not as severe or dangerous in their impacts, can also have important consequences for agriculture and energy demand. They are considered here together with extensive heat waves to provide a more complete picture of variability and trends in summertime temperature extremes over Europe and North America.

We shall see that the regional hot and cold spell indices plainly describe the behavior of regional extreme temperature outbreaks in a way that is complementary to, but fundamentally different from, examinations of temperature magnitudes on local or global scales. One important and robust feature of regional hot and cold spells is their strong low-frequency modulation. Global analyses mask regional decadal variability by averaging over it; local analyses tend to obscure it in higher frequencies. Super-outbreaks of hot and cold air rarely occur counter to prevailing decadal and longer-term trends. Recent trends towards more frequent and extensive hot spells as well as rarer and less extensive cold outbreaks can be explained through a combination of natural multidecadal and anthropogenic influences.

Temperature anomaly magnitude and duration, as well as the spatial extent, of a heat wave all contribute to the severity of its impacts. It is difficult to address all three of these characteristics in one study. Recent studies of heat wave occurrence spurred by the record-breaking 2003 European event focused on the magnitude and duration of *local* temperature anomalies (Beniston, 2004; Beniston and Diaz, 2004; Schar *et al.*, 2004). These studies suggest that the unprecedented temperature anomalies observed at a specific location in connection with the 2003 heat wave were extraordinary with respect to current climate, but were emblematic of expected future conditions. Meehl and Tebaldi (2004), moreover, project that heat waves will become more intense, more frequent, and longer-lasting over Europe and North America in general and specifically at model grid cells around Paris and Chicago. All of these studies examined time slices of several decades in observations and climate models to characterize the effects of anthropogenic climate change projected for an average summer at the end of the twenty-first century. In a rather different study, Stott *et al.* (2004) considered spatially averaged temperatures over the greater Mediterranean region to illustrate that anthropogenic activities have likely increased the risk of an event such as the 2003 European heat wave more than twofold in the current climate, and they projected it to increase 100-fold over the next 40 years. This transition to enhanced heat wave activity over Europe and North America and its dependence on scenarios for political and social action designed to combat global warming, or not, is a major focus of this chapter.

//FS2/CUP/3-PAGINATION/DEX/2-PROOFS/3B2/9780521870283C05.3D 77 [74–98] 19.11.2007 9:27AM

Since large regions (e.g., continents) can and do experience simultaneous subregional hot and cold outbreaks, broad regional temperature averages are not the most appropriate indices for describing variability of regional temperature extremes. In this work, we define an index that *explicitly* reflects the spatial scale of hot and cold outbreaks as well as, although implicitly, their magnitude and duration. The spatial extent of European and North American summertime extreme temperature outbreaks is then considered in the context of decadal and interannual observed variability and coupled model projection of anthropogenic climate change given different scenarios for future emissions and socioeconomic development. Instead of aggregating observed and modeled data in samples of several decades to represent present and future climates as was done in recent studies (Beniston, 2004; Meehl and Tebaldi, 2004; Schar *et al.*, 2004), we present time series of hot and cold spell indices at annual resolution computed for each summer on record – observed and modeled. We then provide a qualitative assessment of the temporal character of spatially extensive temperature extremes over Europe and North America. We consider the extent to which widespread extremes such as the 2003 European event reflect natural climatic variability as opposed to anthropogenic influences. We compare and contrast the recent warming over Europe and North America in the context of their respective regional summer temperature histories and model projections for the future. We discuss the extent to which natural variability is expected to modulate anthropogenic projections of hot and cold extremes over Europe and North America. To better understand the unusual recent summer temperature regime over North America and its likely developments for the near future, we finally focus specifically on the effect of precipitation on regional summer temperatures.

5.2 Regional hot and cold summer indices

We define local heat wave conditions as exhibiting temperatures in the upper 10% of the local climatology over a base period (1950–99). To focus on the spatial extent of heat outbreaks, we construct the regional hot summer index (HSI) by counting the frequency with which each summer (June–July–August, JJA) appears as one of the warmest 10% of summers on the available record at individual locations (stations or grid cells) covering the region of interest. This approach amounts to detecting average summer temperatures warmer than the 90th percentile of the local 1950–99 JJA temperature for all locations over recorded or modeled summers describing a region's climate evolution. The cold summer index (CSI) is constructed similarly for the coldest 10% of summers. Because HSI and CSI (H&CSIs) are computed relative to the local

//FS2/CUP/3-PAGINATION/DEX/2-PROOFS/3B2/9780521870283C05.3D 78 [74–98] 19.11.2007 9:27AM

input data, these indices are insensitive to local systematic biases and extremely robust with respect to the nature of the input data used, as long as the data coverage reasonably represents the region of interest. The locally warmest (coldest) summer, by design, does not have a heavier weighting than the second, third, etc., warmest (coldest) summers on a specific record. The indices are, therefore, very robust with respect to outliers as well as to the spatial detail of heat wave patterns, which may be noisy and/or model specific. But the hot and cold summer indices are designed to be highly sensitive to the *spatial scale* of the individual summer's hot and cold air outbreaks. The H&CSIs efficiently detect interannual variability in spatially extensive extreme temperature outbreaks that are long-lived enough to strongly mark local average JJA temperature. Inasmuch as H&CSIs are sensitive to hot and cold summer extreme temperatures, they are shaped by hot and cold spells. Actual hot and cold *spells* can be quantified more precisely from daily data, and this shall be done in future work. All the same, here we regard the summer indices as reflecting strong and persistent extreme temperature outbreaks. This association can fail during summers marked by hot and cold spells following each other locally in time. However, such summers are highly unusual. It is much more common to have hot and cold spells occurring during the same summer and even simultaneously over different parts of a continent (result not shown). A fundamental difference between H&CSIs and standard regional indices constructed by spatially averaging seasonal temperature anomalies can be appreciated by observing the fact that the H&CSIs perform as intended even when different parts of the region experience opposite temperature extremes.

Of course, H&CSIs are sensitive to the spatial scale of the region of interest and to the percentile of the local temperature climatology chosen to define hot and cold extremes. Both regions considered here are large enough to experience significant hot and cold outbreaks in their different subregions in a specific summer, but also compact enough to allow most of their area to be covered by unusually extensive hot or cold extremes. The temporal structure of H&CSI becomes spikier for smaller regions as well as for more extreme temperature thresholds, more saturated for much larger regions and less extreme percentile thresholds. The main conclusions of this study, however, do not change with the choice of, say, a 75% or 98% threshold for HSI. We apply a 90% JJA temperature threshold as a reasonable compromise between spikiness and saturation.

The new and improved Climatic Research Unit (CRU) observational $5^\circ \times 5^\circ$ gridded surface air temperature, CRUTEM2v (i.e., 2 m air temperature, Ta2m), was used to define past heat wave activity. This monthly global land surface temperature record covers the years 1851–2004 and includes variance

//FS2/CUP/3-PAGINATION/DEX/2-PROOFS/3B2/9780521870283C05.3D 79 [74–98] 19.11.2007 9:27AM

adjustments due to changing station density within each grid box (Jones *et al.*, 1997, 2001). More information on the CRUTEM2v dataset, hereafter referred to as CRU2, can be found in Jones and Moberg (2003). To avoid using values derived from sparse station records, we used data for 1900 on.

Surface air temperatures from 4 coupled global dynamical climate models (CGCMs) out of the 22 available in the IPCC Fourth Assessment simulations database (www-pcmdi.llnl.gov/ipcc) were analyzed. Because our indices are computed relative to regional climatologies, they downplay individual model biases. And since most models show generally similar features of H&CSI behavior relative to their own climatologies, we show results based on one model that is reasonably close to the average of model projections. The CGCM (Douville *et al.*, 2002) is a fully coupled land–ocean–ice–atmosphere dynamical spectral model developed and run at the Centre National de Recherches Météorologiques (CNRM) of Météo France at the spatial resolution of approximately 2.8°. Four integrations of the CGCM have been analyzed. The "historical" run (1860–1999) was forced with observed greenhouse gas and sulfate aerosol concentrations. The "commit" run (2000–2099) is based on concentrations of these gases fixed at the year-2000 level. The SRES-B1 and A2 projections evolve according to different scenarios for socioeconomic development (Arnell *et al.*, 2004). The B1 is a conservative warming scenario that assumes enlightened action by governments to reduce anthropogenic emissions and population growth, while the A1 is essentially "business as usual."

When truly global observational data are required, we use 2 m air temperatures from the National Centers for Environmental Prediction and National Center for Atmospheric Research (NCEP/NCAR) Reanalysis (Kistler *et al.*, 2001) for the period from 1948 to the present. Although known biases exist in these data (Simmonds *et al.*, 2004), they are the most globally complete and physically consistent data available and are adequate for the purposes of this investigation. Reanalysis has a cold bias in surface air temperature owing to the fact that only upper air temperature observations are assimilated, meaning that land use effects are not incorporated. Also, for the period before the late 1970s, the bias is stronger because fewer observations were available for assimilation. Nonetheless, reanalyzed H&CSIs are well correlated with those derived from CRU2.

The different spatial resolutions of the temperature data resulted in 29, 76, and 115 (70, 186, and 354) grid cells available over Europe (North America) from CRU2, CGCM, and reanalysis data, respectively. The close interannual correspondence between H&CSIs derived from CRU2 and reanalysis,[1] two

[1] This correspondence can be seen for Europe in Figure 3.2a.

//FS2/CUP/3-PAGINATION/DEX/2-PROOFS/3B2/9780521870283C05.3D 80 [74–98] 19.11.2007 9:27AM

datasets with vastly different spatial resolutions, provides further evidence of the robustness of our indices with respect to the resolution of the input data.

Near-global gridded station precipitation data (from the Global Historical Climatology Network, GHCN V2) were obtained from the National Climatic Data Center (NCDC); these data consist of observations from 1900 to the present on a 5×5 degree grid (www.ncdc.noaa.gov/oa/climate/research/ghcn/ghcngrid_prcp.html#Overview). All gridded data were weighted by cosine of latitude, although this approach does not significantly affect any of the computed indices.

Over North America, where extensive original and homogenized station temperature and precipitation records are available, results derived from the gridded products (i.e., CRU2, GHCN V2, and Reanalysis), were further validated with an extensive station dataset derived from US (Easterling, 2002; NCDC, 2003; Groisman *et al*., 2004), Mexican (Miranda, 2003), and Canadian (Vincent and Gullett, 1999) networks over North America. In the interest of brevity, we do not show results based on these extensive daily station records here, but we note that the gridded products give essentially the same results. The interesting regional and intraseasonal details that emerge from the station analyses will be presented in future publications.

5.2.1 Europe

Defining Europe by its mid-latitude west-central area as the region situated between 10° W and 25° E, 37° N and 57° N, we first compute the average temperature anomaly from observations and the coupled model relative to their respective 1950–99 climatologies (Figure 5.1a). In contrast to regionally averaged temperatures, which reflect a mixture of magnitude and spatial extent of all seasonal temperature anomalies with coexisting warm and cold anomalies canceling each other, the hot and cold spell indices (H&CSIs, Figure 5.1b) reflect primarily the spatial extent of seasonal warm and cold temperature extremes. Of course, strong coherent anomalies that cover most of the region (i.e., summer 2003) are reflected in both average temperature and in H&CSIs. Regional average temperature, needless to say, is closely correlated with the sum of HSI and CSI, the latter being denoted by negative values as a matter of convention in display. We provide the average temperature anomaly as a reference that shows general temperature tendencies of an entire region, but the H&CSIs provide more detail and will therefore be discussed in greater detail.

The general character of H&CSIs, viewed simultaneously, evolves along with average temperature, but the H&CSI time series are marked with more

//FS2/CUP/3-PAGINATION/DEX/2-PROOFS/3B2/9780521870283C05.3D 81 [74–98] 19.11.2007 9:27AM

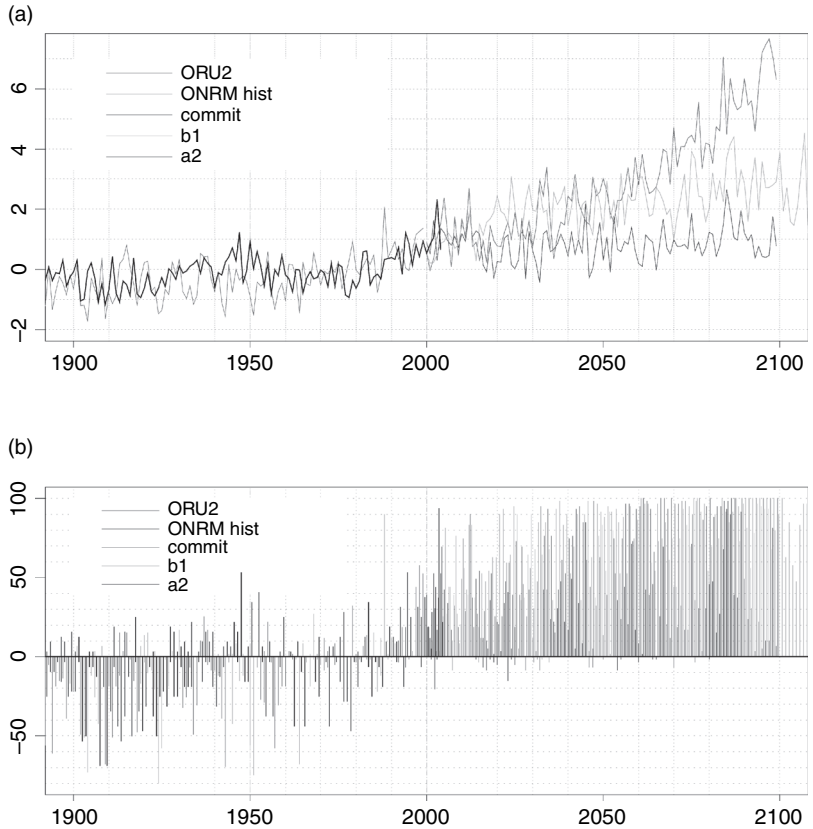

Figure 5.1. (a) European average temperature anomaly relative to the base period 1950–99 from CRU2 observations and the CGCM historical and future scenarios. (b) H&CSIs displayed as percentage of European grid points with summer temperatures above the 90th or below the 10th percentiles of their local summer 1950–99 climatology. HSI (CSI) is displayed in positive (negative) values. By definition, during the base period (delineated by broken orange lines), the mean values are 10% of the area experiencing unusually hot or cold summers. See also Plate 6.

pronounced multidecadal and interannual variability. Apart from several localized heat waves that covered less than a quarter of the area, Europe was predominantly cold until the early 1940s, with the largest cold extremes, affecting almost 70% of the region, occurring in 1907 and 1909. A general warming ensued and, after a few warmer summers, a heat wave occurred in 1947 that covered more than half of Europe. After that, extremes of both signs became more common. However, Europe continued to experience mostly cold summers in the 1950s, 1960s, and 1970s.

The summer of 1976, when approximately 30% of the area experienced hot spell conditions, stands out as the most extreme heat wave since 1952, while the

//FS2/CUP/3-PAGINATION/DEX/2-PROOFS/3B2/9780521870283C05.3D 82 [74–98] 19.11.2007 9:27AM

concurrent cold spell of similar spatial extent seems unremarkable for that period. The 1976 heat wave affected northwestern Europe (Figure 5.2b). It was centered on Great Britain (Green, 1978), where it was the hottest summer on record until 2003 and the cause of much adversity (Subak *et al.*, 2000). However, summer 1976 was actually uncommonly cold over eastern Europe and most of the rest of the northern midlatitudes (Figure 5.2b). The hot and cold spell indices reflect this fact (Figures 5.1b, 5.2a), while the average summer temperature anomaly over the region is close to zero (Figure 5.1a). The case of 1976 accentuates the fact that subregions of a continent or of an entire hemisphere can experience temperature extremes opposite in sign to the prevailing large-scale conditions. It also emphasizes the relative nature of extremes and their impacts viewed in terms of human adaptation to decadal trends. Since the early 1980s, a heat event like that of 1976 was no longer exceptional,[2] with seven hot spells surpassing that of 1976, as well as generally higher mean temperatures. The heat wave of 1994, with over 50% of Europe experiencing heat wave conditions (Figure 5.2a,c), was the most intense event since 1947. The 2003 event[3] was significantly more severe, in terms of both temperature anomaly magnitude and spatial extent (Figures 5.1 and 5.2a,d). Furthermore, no significant cold outbreaks have been experienced since 1993. Viewed in the context of the past century, the heat wave of 2003 is unprecedented. However, it exemplifies the warming trend observed over the last several decades in average summer temperatures as well as in the magnitude and scale of European heat waves (Figures 5.1 and 5.2).

This is part of the warming trend that is manifested globally in the snapshots of Figure 5.2 (b, c, and d), a trend consistent with model projections of anthropogenic warming for Europe and the globe. Even without 2003, European HSIs observed during the past decade indicate the longest and warmest such period on record, a period wholly consistent with the model estimation of warming for anthropogenic forcing fixed at year-2000 levels (the commit run: Figure 5.1a,b).

The coupled model cannot reproduce the observed decadal variability (i.e., the warm late 1940s and early 1950s, the cool late 1970s) – it is not supposed to – but it is able to reproduce the observed warming trend quite well, as do most other coupled models, suggesting an anthropogenic cause to the warming observed since the late 1970s. This being a regional manifestation of a global

[2] Except, of course, from a distinctly British viewpoint.

[3] The 2003 summer heat wave consisted of two outbreaks, one in June and a second in August. Most of the adverse impacts occurred during the second outbreak, when hot anomalies rose above the seasonal temperature maximum in August. For the sake of convenience, we refer to the sum effect of these two outbreaks as reflected in JJA average temperature as the summer 2003 heat wave.

//FS2/CUP/3-PAGINATION/DEX/2-PROOFS/3B2/9780521870283C05.3D 83 [74–98] 19.11.2007 9:27AM

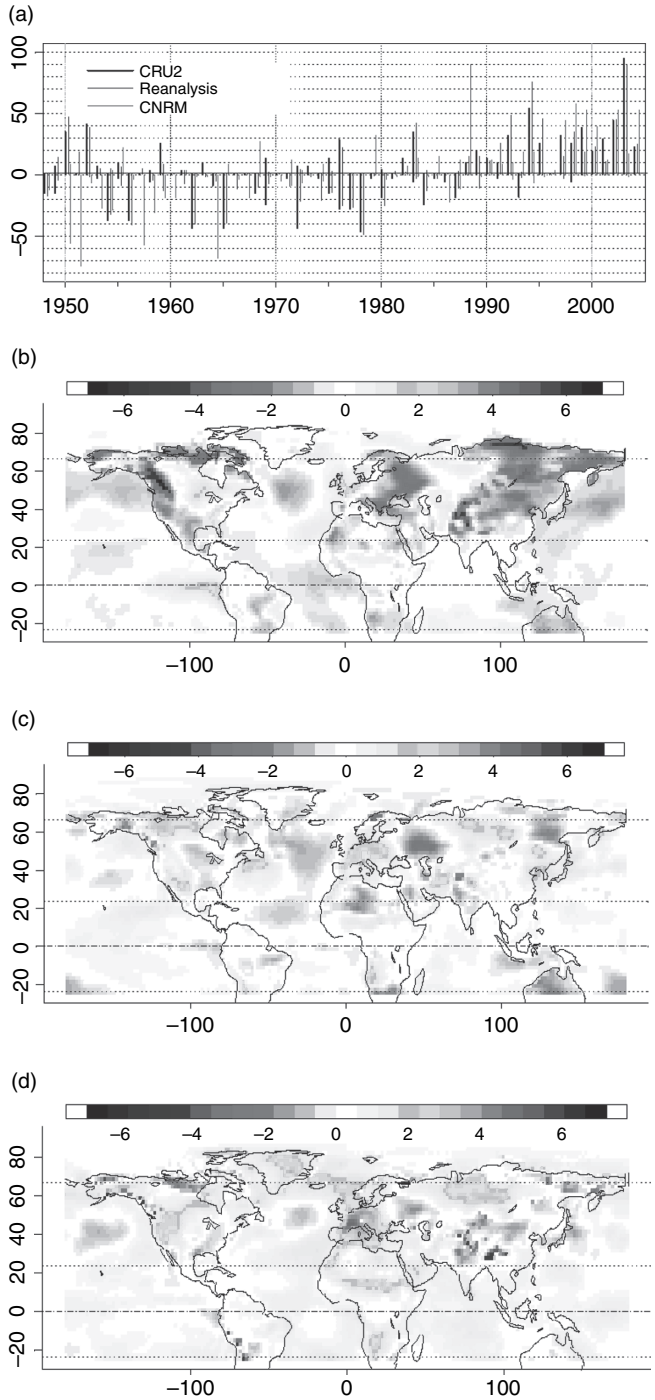

Figure 5.2. (a) H&CSI from CRU2 (black), NCEP/NCAR Reanalysis (red), and CGCM (dashed gray) for the common period 1950–2003. (b) Reanalyzed temperature anomalies for summer 1976, (c) 1994, and (d) 2003. See also Plate 8.

//FS2/CUP/3-PAGINATION/DEX/2-PROOFS/3B2/9780521870283C05.3D 84 [74–98] 19.11.2007 9:27AM

trend, it is difficult to say to what extent natural decadal variability played a part. The historical model run contains one event of the magnitude of 2003 (model year 1988: Figure 5.1b). The CGCM with forcing fixed at year-2000 levels produced three more events of this general magnitude during the twenty-first century. Aided by natural decadal variability, these events all occur in the model during the same decade, the 2080s. Natural decadal variability masks the difference between the two more realistic scenarios (SRES-A2 and B1) in the first half of the twenty-first century, when a 2003-level average temperature becomes common in both model scenarios. Clear differences in scenarios of anthropogenic forcing become apparent in the second half of the century. After the 2050s, 2003-level heat is exceeded in the milder B1 warming scenario in most summers and always in the A2.[4]

Estimating the probabilities of specific events in various time periods and climate change scenarios for Europe involves several problematic assumptions. We prefer to let the reader qualitatively gauge the danger of extremely hot summers in the future by visually examining Figures 5.1 and 5.2.

To place European heat waves into a global temperature context as well as to validate the CGCM, we correlate the HSI with summer surface air temperatures over the globe derived from the Reanalysis and compare these patterns to those derived from the CGCM's commit (i.e., stationary) run (Figure 5.3). Western European heat waves are seasonally correlated with a hemispheric-scale summer temperature wave structure characterized by in-phase behavior over Western Europe and north-central Siberia and out-of-phase behavior over the North Atlantic, European Russia, and the Russian Far East. This is evident in Figure 5.2, but to see it clearly in Ta2 m correlations with HSI, we should remove the observed warming trend from HSI and Ta2 m. Figure 5.3a shows the correlations with the trend present. This approach has the effect of better illustrating European heat wave activity in the context of a warming planet (notice the mostly positive correlations with boreal summer temperatures around the globe) at the expense of masking especially the out-of-phase portions of the Eurasian temperature wave train associated with European heat waves. The wave train correlation structure becomes obvious when the long-term trend is removed from observations (result not shown), and it is well borne out in the commit model run (Figure 5.3b), which is stationary by design. In both the model and observations, there is a strong interannual propensity for western Russia to be cold

[4] According to model results, regional manifestations of global warming should become more evident in the next half century, but differences for varying emissions scenarios (e.g., results of mitigation policies) become discernible only in the second half of the twenty-first century.

//FS2/CUP/3-PAGINATION/DEX/2-PROOFS/3B2/9780521870283C05.3D 85 [74–98] 19.11.2007 9:27AM

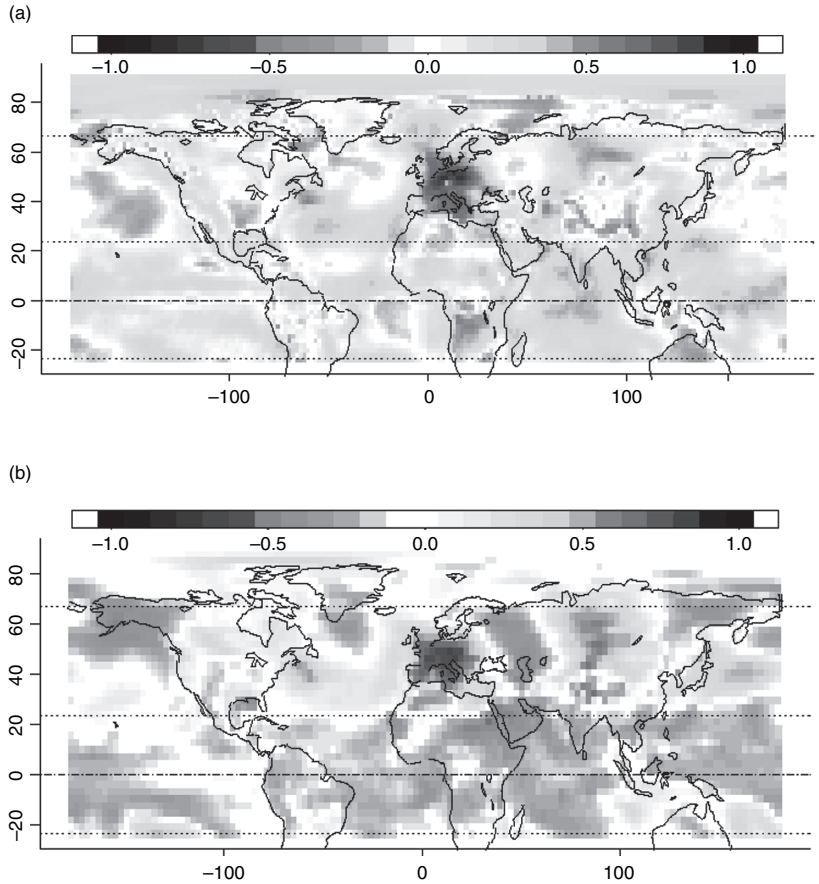

Figure 5.3. Correlation coefficient between Western European HSI and local JJA Ta2 m over the globe in (a) Reanalysis 1948–2003, and (b) the CGCM commit run 2000–99. See also Plate 7.

during heat wave summers in west-central Europe. Both recent extreme European heat wave summers of 1994 and 2003 were cold in western Russia (e.g., anomalous snowfall occurred in Moscow in June 2003; Levinson and Waple, 2004) and warm over north-central Siberia, thus exhibiting Eurasian summer temperature wave train conditions typical of large European heat waves (Figure 5.2c,d).

5.2.2 Midlatitude North America

We limit the study area for North America to the latitudinal band between the Tropic of Cancer and 53° N; north of this band, population and station density becomes sparse, a fact manifested in CRU2 as well as GHCN V2 data gaps

//FS2/CUP/3-PAGINATION/DEX/2-PROOFS/3B2/9780521870283C05.3D 86 [74–98] 19.11.2007 9:27AM

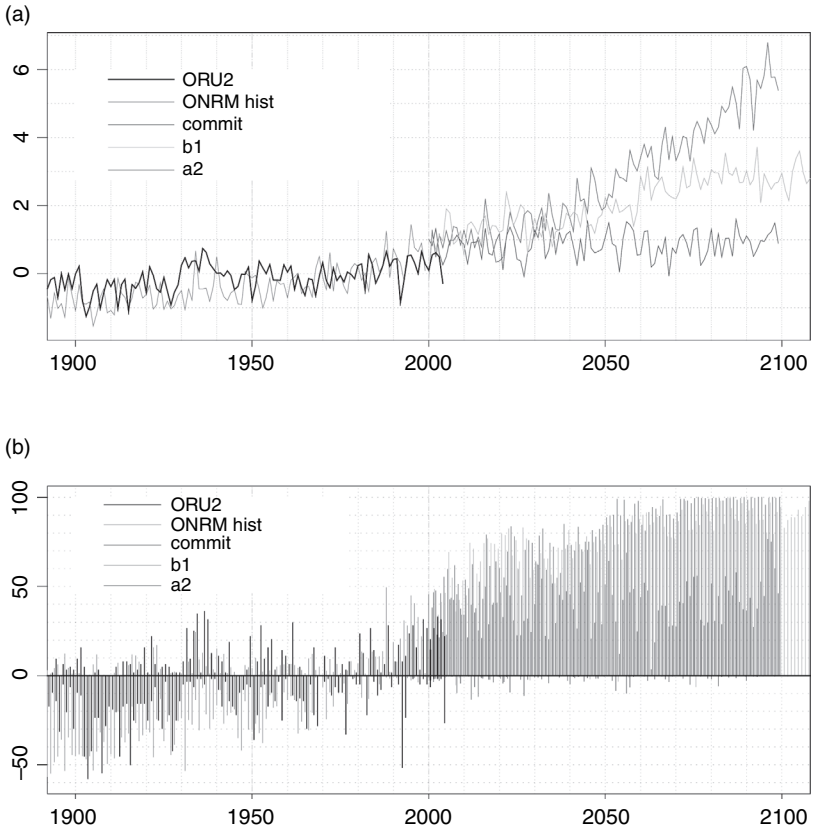

Figure 5.4. Same as Figure 5.1, but for North America; (a) North American average temperature anomaly relative to the base period 1950–99 from CRU2 observations and the CGCM historical and future scenarios. (b) H&CSI displayed as percentage of North American grid points with summer temperatures above the 90th or below the 10th percentiles of their local summer 1950–99 climatology. HSI (CSI) is displayed in positive (negative) values. By definition, during the base period (delineated by broken orange lines), the mean values are 10% of the area experiencing unusually hot or cold summers. See also Plate 9.

over Canada. North American average temperature and H&CSIs derived from observations and the CGCM are displayed in Figure 5.4.

The first three decades of the twentieth century were the coldest on record, with the summers of 1903, 1907, and 1915 experiencing widespread cold anomalies affecting at least one-half of North America, a scale not reached again until 1992 – the largest summer temperature extreme of the second half of the century. We note that these, as well as smaller-scale recent cold outbreaks (e.g., 1976, 1982, 1993, and 2004), were associated with locally wet summers (result not shown). On the other hand, the 1930s appear to have

//FS2/CUP/3-PAGINATION/DEX/2-PROOFS/3B2/9780521870283C05.3D 87 [74–98] 19.11.2007 9:27AM

experienced the warmest and most consistently warm conditions on record, at least until very recently; 7 of 11 (1930–40) summers were more extensively warm (none cool) than expected, and all 11 were warmer than average (see Figure 5.6a for the spatial pattern). The summers of 1934, 1936, and 1937 experienced by far the most severely extensive hot spells of the century (more than 30% of North America was under hot spell conditions). These summers were also exceptionally dry (result not shown for the individual summers; see Figure 5.6b for the 11-year average precipitation anomaly). No summers during the 1930s saw cold outbreaks that even remotely approached their expected spatial extent of 10%.

The 1940s were generally and mildly cool. Temperatures in the 1950s were unusually variable, but the warm summertime temperature anomalies associated with the 1950s drought,[5] although large, were not as spatially extensive, temporally persistent, or exclusive as in the 1930s; they were balanced out by comparably large cold anomalies, a fact reflected in near-zero average temperature anomalies. The 1960s and 1970s saw less variability, with predominantly cool conditions. Temperatures in North America became more variable in the 1980s and 1990s while warming into the start of the twenty-first century. In the midst of general warmth, a cold spell covered 50% of midlatitude North America in 1992, the first time such widespread cold was observed since 1907. The cold summer of 1992 was followed by the mostly cool 1993, both perhaps related to the Mount Pinatubo volcanic eruption[6] (Robock, 2000). But even in the cool summer of 1993 (CSI = 23%), the expected area was hot (HSI = 11%) and the decade that followed (1994–2003) was akin to the 1930s, with 9 out of 10 summers exceeding the mean extent of heat and 3 summers (1998, 2002, and 2003) with hot spell conditions covering more than 30% of the continent for the first time since the 1930s. The last observed summer (2004) was both anomalously warm (HSI = 22%) and cold (CSI = 27%). The recent midwestern heat waves of 1995 and 1999 each resulted in HSI values of under 30%.

The questions as to what global climate conditions are conducive to intense summer heat outbreaks over North America and whether these conditions are reproduced by the model can be addressed by considering maps of correlation coefficients between HSI and local Ta2 m over the globe (Fig. 5.5). In Reanalysis and the CGCM, spatially extensive hot spells over North America

[5] The bulk of the 1950s warmth was coincident with drought, which was mostly concentrated in the fall and winter seasons.

[6] Both these summers, 1992 and 1993, were also anomalously wet over the regions corresponding to the largest observed cooling: Great Plains in 1992, and the northern plains and northwestern United States in 1993 (result not shown). The summer of 1993 was considerably wetter than that of 1992.

//FS2/CUP/3-PAGINATION/DEX/2-PROOFS/3B2/9780521870283C05.3D 88 [74–98] 19.11.2007 9:27AM

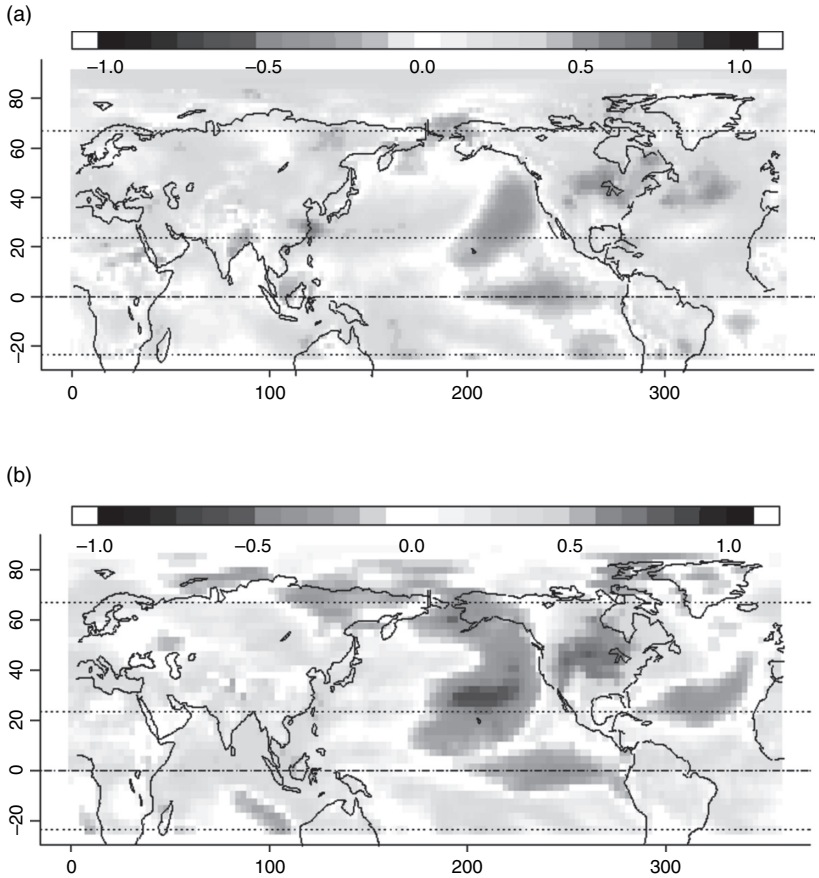

Figure 5.5. Correlation coefficient between North American HSI and local JJA Ta2 m over the globe in (a) Reanalysis, 1948–2003, and (b) the CGCM commit run, 2000–99. See also Plate 10.

tend to organize preferentially around the midwestern United States,[7] and they tend to be associated with cool temperatures in the northeast midlatitude and tropical eastern Pacific, warm temperatures in the subtropical western Pacific, and a general tendency toward warm temperatures in the tropical and northwestern Atlantic. Other patterns apparent in Reanalysis are characterized by

[7] Principal components analysis (PCA) can be used to find coherent patterns of variability that optimally explain the variance of a spatially correlated field; e.g., summer temperature. Principal components analysis applied to CRU2 (as well as to Reanalysis and CGCM) data results in a similar Midwest/Great Plains pattern of summer heat variability (results not shown). Observed H&CSIs are correlated with this main PC mode (correlation = 0.9). This leading mode explains 43% of summer temperature variance (PC2 explains 18%). In CRU2, large peaks (dips) in HSI (CSI) tend to historically line up with those of PC1, indicating that hot (cold) summers tend to have spatially consistent temperature anomalies. The 1930s heat closely followed this pattern. Most other anomalous summers throughout the record did too. Recently, however, the spatial pattern of warming exhibited a rather different structure (see below).

//FS2/CUP/3-PAGINATION/DEX/2-PROOFS/3B2/9780521870283C05.3D 89 [74–98] 19.11.2007 9:27AM

mostly weak positive correlations in patches around the globe, reflecting the general recent global warming. Except for the propensity towards positive correlations dictated by the observed warming trend, the main patterns are reproduced by the model's "commit" climate run, which is stationary by design. The association between HSI and the preferred heat wave location appears to be weakened in Reanalysis, probably because the recent warming over North America did not manifest itself in the preferred heat wave region of the midwestern and north-central United States (see below). Other differences may be due in part to the larger noise level in the shorter reanalyzed climatic sample. As an aside, we have also examined multidecadal changes in global correlation patterns. Modeled correlations computed for consecutive 50-year periods by using the model's historical as well as B1 and A2 runs (figures not shown) plainly resemble the main patterns of Figure 5.5. They also indicate a consistent change in the characteristic pattern of the HSI amounting to a progressive migration of North American heat outbreaks toward the north of the study region. In summary, North American hot summers tend to have a preferred spatial signature that is typically expressed in conjunction with specific sea surface temperature (SST) patterns, and the model appears able to realistically reproduce the observed dynamic structure.

The marine temperature patterns associated with extensive North American summer heat spells are analogous to the anomalous sea surface temperature "forcings" for the 1930s Dust Bowl drought as outlined by Schubert *et al.* (2004). It is also well known that large-scale summer heat can be caused or exacerbated by atmospheric drought through soil moisture deficit (see Alfaro *et al.*, 2006). This was the case in the hot and dry 1930s, when precipitation, especially in summer, was scarce[8] (see Figure 5.6a, b). Although more extreme and persistent than other hot summers on record, the spatial structure of the 1930s heat followed the typical pattern of hot summers over North America (result of PCA not shown). However, the most recent period of summer heat observed over North America, although on the scale approaching that of the 1930s, was not associated either with prolonged large-scale drought or with an anomalously cold tropical Pacific.

In fact, the most recent warm period, 1994–2004, was very much unlike the 1930s (Figure 5.6c). The central and eastern United States were mostly wet over this period[9] (Figure 5.6d). Despite this recent wetness, the central and eastern United States have not cooled as would be naturally expected. Such expectation

[8] Drought reconstructions show that the 1930s Dust Bowl drought was the most severe and widespread such event to strike the United States since 1700 (Cook *et al.*, 1999).

[9] In fact, the entire country has been generally wet over the last quarter century.

//FS2/CUP/3-PAGINATION/DEX/2-PROOFS/3B2/9780521870283C05.3D 90 [74–98] 19.11.2007 9:27AM

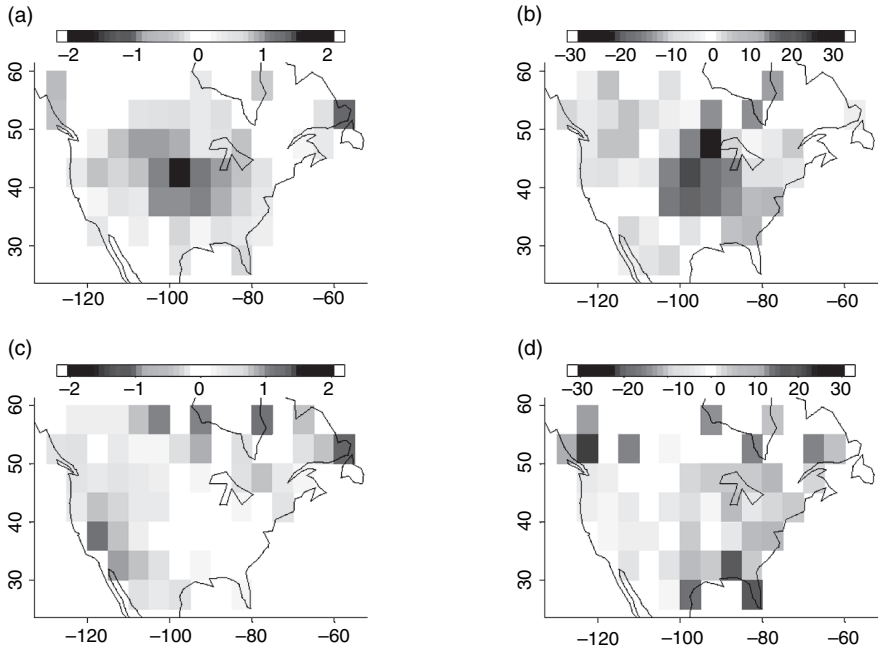

Figure 5.6. Summer temperature (a, c) and precipitation (b, d) anomalies for two 11-year periods: 1930–1940 (a, b) and the most recent period of record, 1994–2004 (c, d). Notice the reversed color scale on the precipitation plots. Canadian precipitation records suffer from missing data at the end of the record, accounting for the visible discontinuity along the US–Canada border in (d). See also Plate 11.

is supported by Figure 5.7a, which shows observed local correlations between summer temperatures and precipitation. Meanwhile, much of the recent warming over midlatitude North America has been due to warmer summers all around this central and eastern US wet spot (Figure 5.6c,d). Recent summer warmth over California and the rest of the mountainous West is probably related to the strong warming observed in the West during winter and spring, which resulted in changes in the snow-to-rain ratio (Knowles *et al.*, 2006) as well as the spring's earlier arrival and related changes in surface hydrology (Cayan *et al.*, 2001), drying the soil in summer without appreciable changes in precipitation amounts. These same changes in summer temperatures and hydrology have also resulted in increased wildfire activity over the western mountains (Westerling *et al.*, 2006). The western summer warming (Figure 5.6c) is reflected in increasing values of the North American HSI, but this pattern is generally atypical of extensive North American summer heat.

Strong and extensive Canadian warming, apparent in Figure 5.6c, did not strongly affect the earlier results because only far southern Canadian data, for

//FS2/CUP/3-PAGINATION/DEX/2-PROOFS/3B2/9780521870283C05.3D 91 [74–98] 19.11.2007 9:27AM

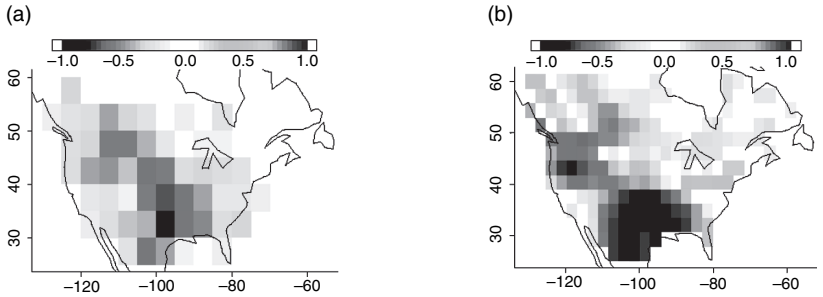

Figure 5.7. Correlation coefficient between local June–August average temperature and precipitation in (a) observations (GHCN V2 and CRU2 evaluated over the period of record, 1900–2004, or slightly shorter based on data availability for the individual grids) and (b) the model (the commit run, 100 years). See also Plate 11.

reasons of data quality given above, were included in the North American index calculation. Had more extensive Canadian data been included, the recent warming would have appeared larger. This observation is consistent with the model result projecting heat waves to spread progressively towards the north (not shown).

5.3 Role of precipitation

There is a well-known interaction between soil moisture and surface level temperature. On the one hand, anomalous prolonged warmth can desiccate the soil; on the other, the drier the soil, the less energy is required to heat it. Precipitation deficit can, therefore, enhance regional heat wave activity and partially account for multidecadal timescales in extreme summer heat outbreaks that can temporarily either promote or dampen the effects of global warming. Summer heat and precipitation are, of course, dynamically linked, for the anticyclonic circulation that produces heat waves also precludes precipitation. In regions that typically receive much summer precipitation, it is therefore difficult to isolate the effect of contemporaneous (summer) precipitation on temperature. The effect of antecedent precipitation on summer temperature through soil moisture accumulation is typically small and may influence heat waves, primarily in the early summer. In regions where summer precipitation amounts are small, and especially where winter precipitation is stored as snowpack (e.g., California and the mountainous Southwest), the delayed precipitation–soil moisture effect can be much stronger.

We have examined the contemporaneous and lagged relationships between local summer temperature and precipitation. Figure 5.7 shows that the two

//FS2/CUP/3-PAGINATION/DEX/2-PROOFS/3B2/9780521870283C05.3D 92 [74–98] 19.11.2007 9:27AM

are strongly anticorrelated over North America,[10] particularly along the Front Range of the Rockies and to the southeast over the Great Plains and over a great part of the Midwest and the Gulf Coast, the Mexican Plateau, and the mountainous northwestern United States. We have also regressed precipitation out of local summer temperature and compared resulting regionally averaged temperatures as well as H&CSI with raw values discussed above over both Europe and North America. These results are not shown, but they indicate that precipitation deficit appears to have played a critical role in enhancing the severity of Europe's 2003 heat wave as well as the Dust Bowl and other observed extremes. However, the bulk of the recent observed warming trend over Europe is not associated with drying.[11] Moreover, the area that traditionally experiences large-scale heat waves, the Midwest and Great Plains region of the United States, has remained close to normal (Figure 5.6c). In this area and to the south and west of it, summer temperature is strongly anticorrelated with precipitation (Figure 5.7a). It is important to emphasize that this has been true historically on interannual as well as longer timescales, but lately, the local anticorrelation on decadal timescales has disappeared. Although the central/eastern United States has been unusually wet in recent decades, no significant long-term cooling has occurred there. Rather, normal conditions have prevailed in this region recently. The laws of thermodynamics require us to assume that there has been a concurrent warming that has offset the cooling expected in the central and eastern United States in response to increased wetness. Giving further support to this inference, the rest of North America has most certainly warmed. If this background warming persists or continues, as we can expect from model results (see Figure 5.4 as well as results of numerous other modeling studies), we can reasonably expect that the end of the current wet spell should be accompanied by stronger and more extensive summer warmth over the central and eastern United States.

As for the model, the regions of largest projected midlatitude continental summer warming in both the A2 and B1 scenarios are those with projected regional decreases in precipitation (result not shown). This is not surprising. The model is certainly able to reproduce the spatial signature of the local summertime precipitation–temperature relationship, albeit with somewhat stronger than observed coupling (Figure 5.7b).

[10] Europe presents a similar picture, but the anticorrelation is somewhat weaker than it is for North America.

[11] Rather, it appears to be associated with the enhanced greenhouse effect of water vapor (Philipona *et al.*, 2005).

//FS2/CUP/3-PAGINATION/DEX/2-PROOFS/3B2/9780521870283C05.3D 93 [74–98] 19.11.2007 9:27AM

5.4 Summary and conclusions

Examination of hot and cold summer indices over continental-scale regions suggests that in practically every summer there is a temperature extreme somewhere (Figures 5.1b and 5.4b). The European HSI shows the 2003 event to be the most intense and widespread since the beginning of record. According to our definition, more than 90% of western and central Europe experienced hot spell conditions in 2003. At many European locations, 2003 was the hottest summer on record, probably the hottest in over 500 years (Luterbacher *et al.*, 2004), with average summer temperature anomalies reaching 5 °C (Figure 5.2d). This intensely and extensively hot summer was consistent with the multidecadal warming trend towards more frequent and extensive European heat waves apparent since the late 1970s (Figure 5.1b). Coupled model projections show a combination of natural and anthropogenic influences, with their relative magnitudes being a function of the particular scenario assumed for global socioeconomic development: i.e., resolute action or inaction on the part of nations. For now, Europe appears to have had an early warning in 2003 of conditions projected for the second half of the twenty-first century, assuming inaction. This conclusion is consistent with those of other recent studies (Beniston, 2004; Beniston and Diaz, 2004; Meehl and Tebaldi, 2004; Schar *et al.*, 2004; Stott *et al.*, 2004). Drought certainly enhanced the severity of the 2003 event (Levinson and Waple, 2004). Apart from this, drought does not appear to have been a general factor in the recently observed warming trend. Fresh observational evidence suggests that much of the recent warming over Europe, at least around the Alps, has been caused by the enhanced greenhouse effect due to water vapor feedback (Philipona *et al.*, 2005) – water vapor being the most important and variable greenhouse gas. For now, Europe is warming at least as much and as fast as predicted by the climate model.

North America, while also warming, has not yet felt the feasible level of heat projected for the current stage of anthropogenic climate change. Interestingly, the current warm period, although at least in spatial extent comparable with the 1930s Dust Bowl, does not involve the same region of North America and is not associated with severe drought; it is, therefore, very much unlike the similar-scale 1930s warming (and other more common warm events). The recent summertime warming over North America has occurred notably in the mountainous West, where it is consistent with observed hydrological changes initiated by warming trends in the winter and spring. Specifically, the western summertime warming occurred alongside a strong observed trend towards warmer winters and springs and earlier snowmelt (Cayan *et al.*, 2001), as well

//FS2/CUP/3-PAGINATION/DEX/2-PROOFS/3B2/9780521870283C05.3D 94 [74–98] 19.11.2007 9:27AM

as decreasing snow/rainfall ratios (Knowles *et al.*, 2006). The hydrological changes initiated by these trends in winter and spring result in drying of the soil into the summertime and can partially explain the western summertime warming. It is possible that European-Alpine-type water vapor feedback processes (see Philipona *et al.*, 2005) may also explain a part of this western summertime warming. Supporting such a possibility, as well as giving further verification of a large-scale environmental change, is the fact that North American warming also has a broad Canadian footprint (Figure 5.6c). However, Canadian data were mostly excluded from index calculations here.

The only portion of North America that has not warmed lately is the central and eastern United States, a preferred area for heat wave occurrence and an area where summer temperature and precipitation are strongly anticorrelated; i.e., this region has high drought-related heat wave potential. The anomalous recent wetness over this region would be normally associated with cool summers, but the region has experienced average temperatures recently. These observations point to global warming as a likely cause for the *lack* of cooling over the central and eastern United States over the last couple of decades. In other words, natural decadal variability associated with precipitation appears to be at work taking the edge off the anthropogenic warming over the central and eastern United States. This means that the next large-scale Great Plains summer drought will likely be associated with warming exceeding that of the 1930s in both magnitude and spatial extent. For the same reason, a mega-drought of 1930s intensity and spatial extent no longer appears to be required to produce heat wave activity on the scale of the Dust Bowl. A more pedestrian drought will do.

The CGCM driven with anthropogenic forcing reproduces well the warming observed over Europe and North America. It also reproduces well the coupling of summertime temperature and precipitation. Model results interpreted in light of the observations suggest that, even at anthropogenic output fixed at current levels, we can expect much stronger and more widespread heat waves than have been observed up to now in North America as soon as natural decadal variability (e.g., precipitation) turns to conspire with, or at least stops counteracting, the anthropogenic signal. The model also provides variants of likely further evolution of summer heat. The A2 and B1 warming scenarios are indistinguishable from each other in the next several decades mostly because each model run is strongly modulated by its own natural decadal variability. However, by the middle of the century, the two scenarios clearly diverge, with the B1 stabilizing at a temperature anomaly of about 3 °C and HSI between 75% and 98%, while the A2 saturates at HSI = 100% by about 2070 with temperatures continuing to rise.

//FS2/CUP/3-PAGINATION/DEX/2-PROOFS/3B2/9780521870283C05.3D 95 [74–98] 19.11.2007 9:27AM

Our results agree with recent studies in general, and they complement these studies by providing a time-evolving view of regional heat wave activity in individual summers that naturally emphasizes higher-frequency variability on top of the anthropogenic trend. Moreover, our explicit focus on the heat wave's spatial extent emphasizes the European 2003 heat wave type – as well as that of 1934 and 1936, the Dust Bowl's defining years – over much smaller-scale heat waves (such as the more recent Midwestern heat waves of 1995 and 1999). Our results further identify the central, midwestern, and eastern United States as the regions most at risk of "surprise" intensification of summer heat wave activity. These regions are traditionally prone to heat waves, but they have been cooled off recently by unusually wet conditions, which cannot be expected to persist much longer.

Over North America, a spatially extensive heat wave of the magnitude of Europe 2003 has not occurred in observed history. However, the probability of such an event may be significant and increasing. The observed current level of warming agrees with the cooler decades projected by the model run with anthropogenic forcing fixed at current levels. However, even with this fixed forcing, 22% of the projected heat waves cover over half of North America, a level heretofore not reached in observations. Realistically, this level and spatial extent of summer heat, were it to occur in the near future and in its preferred location, will be coupled with drought. It is clear that if such extensively hot and dry summers were to occur in reality, especially if they were unanticipated, would produce adverse consequences for North America. Observational and model results both suggest, furthermore, that such extremes exhibit natural cycles and tend to congregate in decadal sequences of hot summers.

Public perception of climate variability and change is strongly influenced by seasonal extremes. For example, the summers of 1976–78 experienced extremely cold conditions over widespread northern midlatitude regions even when considered in the context of the 1960s and 1970s, two consistently cold decades. It is not surprising, therefore, that three decades ago, the actual concern was global cooling (Kukla *et al*., 1977), although no plausible mechanisms for such cooling were identified. Timescales are easily confused, however, and, at least in nonscientific literature, this strong decadal variation was at the time widely taken for the beginning of an ice age (Ponte, 1976). Conversely, the last two decades of the twentieth century experienced a mean warming trend globally and over the midlatitude Northern Hemisphere unprecedented in recent centuries (Mann *et al*., 1998; Moberg *et al*., 2005), a trend that continues strongly up to the present (Hansen *et al*., 2006; Jones and Palutikof, 2006). This recent warming was punctuated by increasing frequencies of large-scale regional hot summer outbreaks and a decrease in the frequencies of cold

//FS2/CUP/3-PAGINATION/DEX/2-PROOFS/3B2/9780521870283C05.3D 96 [74–98] 19.11.2007 9:27AM

summers. Plausible mechanisms for such a trend do exist and are exemplified by the IPCC socioeconomic and emissions scenarios (Arnell *et al*., 2004). Further anthropogenic warming accompanied by more frequent, intense, and extensive heat waves is projected, but, owing to natural decadal-scale climate variability, it appears that regional effects of global policy action (e.g., "business as usual" vs. "enlightened management" scenarios) may not be detectable for several decades ahead. Of course, although the probability of regional-scale cold outbreaks is expected to diminish over this century, they are still possible and will occur with a generally decreasing frequency and spatial extent. However, cold outbreaks will certainly occur frequently enough to spur outbreaks of regional skepticism regarding the nature and causes of climatic change for several decades to come.

Acknowledgments

The original ideas and research presented here were initiated during Gershunov's visit to CNRM in the summer of 2004. This visit was supported by Météo France through the visiting scholar program. We thank Sophie Tyteca and Mary Tyree for help with data acquisition and processing. Partial funding was provided by the California Climate Change Center, sponsored by the California Energy Commission's Public Interest Energy Research Program and by the NOAA Office of Global Programs, under the California Applications Program.

References

Alfaro, E., Gershunov, A., and Cayan, D. R. (2006). Prediction of summer maximum and minimum temperature over the central and western United States: the role of soil moisture and sea surface temperature. *Journal of Climate*, **19**, 1407–27.

Arnell, N. W., Livermore, M. J. L., Kovats, S., *et al*. (2004). Climate and socio-economic scenarios for global-scale climate change impacts assessments: characterising the SRES storylines. *Global Environmental Change: Human and Policy Dimensions*, **14**, 3–20.

Ballester, F., Michelozzi, P., and Iniguez, C. (2003). Weather, climate, and public health. *Journal of Epidemiology and Community Health*, **57**, 759–60.

Beniston, M. (2004). The 2003 heat wave in Europe: a shape of things to come? An analysis based on Swiss climatological data and model simulations. *Geophysical Research Letters*, **31**, L02202, doi:10.1029/2003GL018857.

Beniston, M., and Diaz, H. F. (2004). The 2003 heat wave as an example of summers in a greenhouse climate? Observations and climate model simulations for Basel, Switzerland. *Global and Planetary Change*, **44**, 73–81.

Cayan, D. R., Kammerdiener, S. A., Dettinger, M. D., Caprio, J. M., and Peterson, D.H. (2001). Changes in the onset of spring in the western United States. *Bulletin of the American Meteorological Society*, **82**, 399–415.

//FS2/CUP/3-PAGINATION/DEX/2-PROOFS/3B2/9780521870283C05.3D 97 [74–98] 19.11.2007 9:27AM

Cook, E. R., Meko, D. M., Stahle, D. W., *et al*. (1999). Drought reconstructions for the continental United States. *Journal of Climate*, **12**, 1145–62.
Dhainaut, J. F., Claessens, Y. E., Ginsburg, C., and Riou, B. (2004). Unprecedented heat-related deaths during the 2003 heat wave in Paris: consequences on emergency departments. *Critical Care*, **8**, 1–2.
Douville, H., Chauvin, F., Royer, J. -F., Salas-Mélia, S., and Tyteca, S. (2002). Sensitivity of the hydrological cycle to increasing amounts of greenhouse gases and aerosols. *Climate Dynamics*, **20**, 45–68.
Easterling, D. R. (2002). Recent changes in frost days and the frost-free season in the United States. *Bulletin of the American Meteorological Society*, **83**, 1327–32.
Green, F. H. W. (1978). Exceptional heat-wave of 23 June to 8 July 1976. *Meteorological Magazine*, **107**, 99–100.
Groisman, P. Y., Knight, R. W., Karl, T. R., *et al*. (2004). Contemporary changes of the hydrological cycle over the contiguous United States: trends derived from in-situ observations. *Journal of Hydrometeorology*, **5**, 64–85.
Hansen, J., Ruedy, R., Sato, M., and Lo, K. (2006). Global temperature trends: 2005 summation. (http://data.giss.nasa.gov/gistemp/2005/).
Jones, P. D., and Moberg, A. (2003). Hemispheric and large-scale surface air temperature variations: an extensive revision and an update to 2001. *Journal of Climate*, **16**, 206–23.
Jones, P. D., and Palutikof, J. (2006). Global temperature record. (www.cru.uea.ac.uk/cru/info/warming/).
Jones, P.D., Osborn, T.J. and Briffa, K.R. (1997). Estimating sampling errors in large-scale temperature averages. *Journal of Climate*, **10**, 2548–68.
Jones, P. D., Osborn, T. J., Briffa, K. R., *et al*. (2001). Adjusting for sampling density in grid-box land and ocean surface temperature time series. *Journal of Geophysical Research*, **106**, 3371–80.
Kistler, R., Kalnay, E., Collins, W., *et al*. (2001). The NCEP-NCAR 50-year reanalysis: monthly means CD-ROM and documentation. *Bulletin of the American Meteorological Society*, **82**, 247–67.
Knowles, N., Dettinger, M. D., and Cayan, D. R. (2006). Trends in snowfall versus rainfall in the western United States. *Journal of Climate*, **19**, 4545–59.
Kukla, G. J., Angell, J. K., Korshover, J., *et al*. (1977). New data on climatic trends. *Nature*, **270**, 573–80.
Levinson, D. H., and Waple, A. M. (2004). State of climate in 2003. *Bulletin of the American Meteorological Society*, **85**, 1–72.
Luterbacher, J., Dietrich, D., Xoplaki, E., Grosjean, M., and Wanner, H. (2005). European seasonal and annual temperature variability, trends, and extremes since 1500. *Science*, **303**, 1499–503.
Macfarlane, A., and Waller, R.E. (1976). Short-term increases in mortality during heat waves. *Nature*, **264**, 434–6.
Mann, M. E., Bradley, R. S., and Hughes, M. K. (1998). Global-scale temperature patterns and climate forcing over the past six centuries. *Nature*, **392**, 779–87.
Meehl, G. A., and Tebaldi, C. (2004). More intense, more frequent, and longer lasting heat waves in the twenty-first century. *Science*, **305**, 994–7.
Miranda, S. (2003). Actualizacion de la base de datos ERIC II. Final report of the project TH-0226, Instituto Mexicano de Tecnología y Agua (IMTA) internal reports.
Moberg A., Sonechkin, D. M., Holmgren, K., Datsenko, N. M., and Karlén, W. (2005). Highly variable Northern Hemisphere temperatures reconstructed from low- and high-resolution proxy data. *Nature*, **433**, 613–17.

//FS2/CUP/3-PAGINATION/DEX/2-PROOFS/3B2/9780521870283C05.3D 98 [74–98] 19.11.2007 9:27AM

National Climatic Data Center (NCDC). (2003). Data documentation for data set 3200 (DSI-3200), Surface land daily cooperative summary of the day. Asheville, North Carolina: National Climatic Data Center, 36 pp. (Available online at www.ncdc.noaa.gov/pub/data/documentlibrary/tddoc/td3200.pdf.)

Palecki, M. A., Changnon, S. A., and Kunkel, K.E. (2001). The nature and impacts of the July 1999 heat wave in the midwestern United States: learning from the lessons of 1995. *Bulletin of the American Meteorological Society*, **82**, 1353–67.

Philipona, R., Dürr, B., Ohmura, A., and Ruckstuhl, C. (2005). Anthropogenic greenhouse forcing and strong water vapor feedback increase temperature in Europe. *Geophysical Research Letters*, **32**, L19809, doi:10.1029/2005GL023624.

Ponte, L. (1976). *The Cooling*. Englewood Cliffs, NJ: Prentice-Hall.

Robock, A. (2000). Volcanic eruptions and climate. *Reviews of Geophysics*, **38**, 191–219.

Schar, C., Vidale, P. L., Luthi, D., *et al.* (2004). The role of increasing temperature variability in European summer heat waves. *Nature*, **427**, 332–6.

Schubert, S. D., Suarez, M. J., Pegion, P. J., Koster, R. D., and Bacmeister, J. T. (2004). On the cause of the 1930s Dust Bowl. *Science*, **303**, 1855–9.

Sheridan, S. C., and Kalkstein, L. S. (2004). Progress in Heat Watch–Warning System technology. *Bulletin of the American Meteorological Society*, **85**, 1931–41.

Simmonds, A. J., Jones, P. D. da Costa Bechtold, V., *et al.* (2004). Comparison of trends and variability in CRU, RTA-40 and NCEP/NCAR analyses of monthly-mean surface air temperature. ERA-40 Project Report Series No. 18.

Stott, P. A., Stone, D.A., and Allen, M. R. (2004). Human contribution to the European heat wave of 2003. *Nature*, **432**, 610–13.

Subak, S., Palutikof, J. P., Agnew, M. D., *et al.* (2000). The impact of the anomalous weather of 1995 on the U.K. economy. *Climatic Change*, **44**, 1–26.

Vincent, L. A., and Gullett, D. W. (1999). Canadian historical and homogeneous temperature datasets for climate change analyses. *International Journal of Climatology*, **19**, 1375–88.

Westerling, A. L., Hidalgo, H. G., Cayan, D. R., and Swetnam, T. W. (2006). Warming and earlier spring increase western U.S. forest wildfire activity. *Science*, **313**, 940–3.

Zell, R. (2004). Global climate change and the emergence/re-emergence of infectious diseases. *International Journal of Medical Microbiology*, **293**, 16–26.